Geotextiles and Geomembranes 47 (2019) 128–139

Contents lists available at ScienceDirect

Geotextiles and Geomembranes

journal homepage: www.elsevier.com/locate/geotexmem

Strength enhancement of geotextile-reinforced carbonate sand

Saeed Goodarzi, Habib Shahnazari*

School of Civil Engineering, Iran University of Science and Technology, P.O. Box 16765-163, Narmak, Tehran, Iran

ARTICLE INFO

Keywords:
Geosynthetics
Shear behavior
Carbonate sand
Geotextile
Triaxial test
Sand reinforcement

ABSTRACT

The mechanical behavior of carbonate sand reinforced with horizontal layers of geotextile is invetigated using a series of drained compression triaxial tests on unreinforced and reinforced samples. The main factors affecting the mechanical behavior such as the number of geotextile layers, their arrangement in specimens, confining pressure, particle size distribution, geotextile type and relative density of samples were examined and discussed in this research. To make a precise comparison between the behavior of reinforced siliceous and carbonate sand, triaxial tests were performed on both types of sands. Results indicate that geotextile inclusion increases the peak strength and strain at failure, and significantly reduces the post-peak strength loss of carbonate specimens. The amount of strength enhancement rises as the number of geotextile layers increases while two other parameters including confining pressure and particle size affect adversely. The strength enhancement of reinforced carbonate sand is greater than the corresponding siliceous sample at high axial strains. Reinforced and unreinforced carbonate specimens exhibit more contractive behavior than their corresponding siliceous samples and tend to dilate at higher axial strains. By increasing the relative density of the samples, the peak strength of reinforced specimens rises due to enhanced interlocking between geotextile layers and sand particles. This process continues as long as the geotextile is not ruptured. The utilization of geotextiles with high mass per unit areas was found to be uneconomical due to slight differences between the strength augmentation of geotextiles with high and low mass per unit areas. It should be noted that geotextile layers limit the lateral expansion of specimens which leads to changing the failure pattern from a shear plane to bulging between the adjacent layers of geotextile.

1. Introduction

Carbonate sediments can be found in temperate and tropical areas (e.g., the Persian Gulf of Iran, Hawaiian Islands, Puerto Rico, Republic of Ireland, and Australia). Development and geotechnical construction in these regions have been significantly improved in recent years due to the existence of petrochemical reserves and tourism. Many studies indicate that the mechanical behavior of carbonate sands is different from siliceous sands (Brandes, 2011; Celestino and Mitchell, 1983; Coop, 1990; Datta et al., 1979; Jafarian et al., 2018a; Rezvani et al., 2011; Shahnazari et al., 2016a; Shahnazari and Rezvani, 2013). There are two primary reasons account for the differences between carbonate and siliceous sands. First, carbonate sands contain shells and coral particles that have cavities inside their bodies, resulting in significant intraparticle void space (within the particles) (Golightly, 1988; Hyodo et al., 1996; Sharma and Ismail, 2006). Second, carbonate sands have considerable inter-particle space (between particles) which is attributed to various shapes of carbonate particles (Salem et al., 2013). Both reasons give rise to the higher compressibility potential of carbonate sands associated with crushing of carbonate particles when sheared (Shahnazari et al., 2016b). Therefore, results of studies conducted on geosynthetic reinforced siliceous sands cannot be generalized to carbonate sands.

Geotextiles have been widely utilized in various geotechnical engineering projects such as roads, residences, slope stabilizations, bridge abutments, and landfills (Kalpakci et al., 2018; Kermani et al., 2018; King et al., 2017; Rowe et al., 2016; Rowe and Liu, 2015; Saran and Viswanadham, 2018; Zheng and Fox, 2017; Zornberg et al., 2017). Diverse experimental approaches were utilized to investigate the productive effects of geotextile reinforcement in geotechnical projects. Some researchers employed full-scale models to evaluate the effects of reinforced horizontal geosynthetic layers in soil (Liao and Su, 2012; Perkins and Cortez, 2005; Plácido et al., 2018; Portelinha and Zornberg, 2017; Wang et al., 2018; Zornberg et al., 2013). Reduced-scale experiments are more prevalent than full-scale experiments due to the arduous construction of full-scale models. Several available studies employed reduced-scale models of geotextile-reinforced soil (Chi et al., 2012; Costa et al., 2016; Guler and Selek, 2014; Luo et al., 2018; Nova-

* Corresponding author.
E-mail address: hshahnazari@iust.ac.ir (H. Shahnazari).

https://doi.org/10.1016/j.geotexmem.2018.12.004
Received 12 August 2018; Received in revised form 7 December 2018; Accepted 10 December 2018

Roessig and Sitar, 2006; Turker et al., 2014; Yang et al., 2012; Zornberg and Arriag, 2003). The other experimental approach to investigate the effect of geotextile reinforcement is utilizing element tests by apparatus such as compression triaxial and direct shear equipment (Afzali-Nejad et al., 2017; Denine et al., 2016; Latha and Murthy, 2006; Ziaie Moayed and Alibolandi, 2018).

Gray and Al-Refeai (1986) carried out a series of monotonic compression triaxial tests on dry sand reinforced with horizontal layers of geotextile. Results indicated that geotextile inclusion increased the peak strength and axial strain at failure. Haeri et al. (2000) used samples with various numbers of geotextile layers and different diameters to investigate the behavior of sand reinforced with geotextile. They illustrated that increasing the number of geotextile layers increased the peak strength and ductility; the amount of improvement was more noticeable in the smaller samples. Latha and Murthy (2007) reinforced sand with three different forms of horizontal geosynthetics, geocell and discrete fibers. Unreinforced and reinforced samples were studied by triaxial compression tests to investigate the effect of various forms of reinforcement. Results indicated that all three forms of reinforcement strengthened the sand, but the strength increment in geocell was more than the other two forms. Nguyen et al. (2013) conducted a series of monotonic triaxial tests on sand reinforced with horizontal layers of geotextile. They retrieved geotextiles from samples after the test process and investigated them with an image-processing technique. They observed that the maximum strain of geotextile was situated at its center and decreased along the radial direction. They also indicated that geotextile layers required sufficient deformation to mobilize their tensile force for enhancing the shear strength of specimens. They revealed that geotextile reinforcement at axial strains lower than 1–3% not only did not increase the shear strength, but also decreased it. Naeini and Gholampoor (2014) studied the effect of silt inclusion in geotextile reinforced samples with cyclic triaxial tests. Results demonstrated that employing geotextiles decreased the cyclic ductility of dry sand. Increasing silt content up to 35% resulted in a decrease in the sample strength, but a further increase in silt content enhanced the sample strength. Benessalah et al. (2016) conducted a series of triaxial tests on medium and dense specimens; they concluded that reinforcement had more effect on dense samples than medium samples. Latha and AM (2016) performed static and dynamic large-scale triaxial tests on geosynthetic-reinforced samples to overcome boundary condition. Results indicated an increment in the peak strength, strain at failure, and stiffness under static conditions and also an increase in the dynamic moduli under dynamic conditions. Markou (2018) used direct shear and triaxial tests to study the effect of particle shape and size on the sand-geotextile interaction. He detected that rounded and fine sand particles were able to mobilize the friction of soil-geotextile interface more effectively than other particles.

Although extensive studies have been conducted to investigate the behavior of siliceous sand reinforced with geotextile, no experiment was carried out on geotextile reinforced carbonate sand. In this study, a series of compression triaxial tests were conducted on both siliceous and carbonate sand reinforced with horizontal geotextile layers to compare the effects of geotextile inclusion in both types of sands at different levels of axial strain. Geotextile-reinforced specimens were tested while varying the number and arrangement of geotextile layers, the relative density of soil, types of geotextile, particle size distribution, and confining pressure.

2. Test materials

2.1. Soil

Carbonate sand utilized in this research was obtained from the northwest coast of Hormoz Island in the Persian Gulf; it should be noted that the sand was not cemented. Settlements were observed in some old and new buildings on this island, which indicate the compressibility of

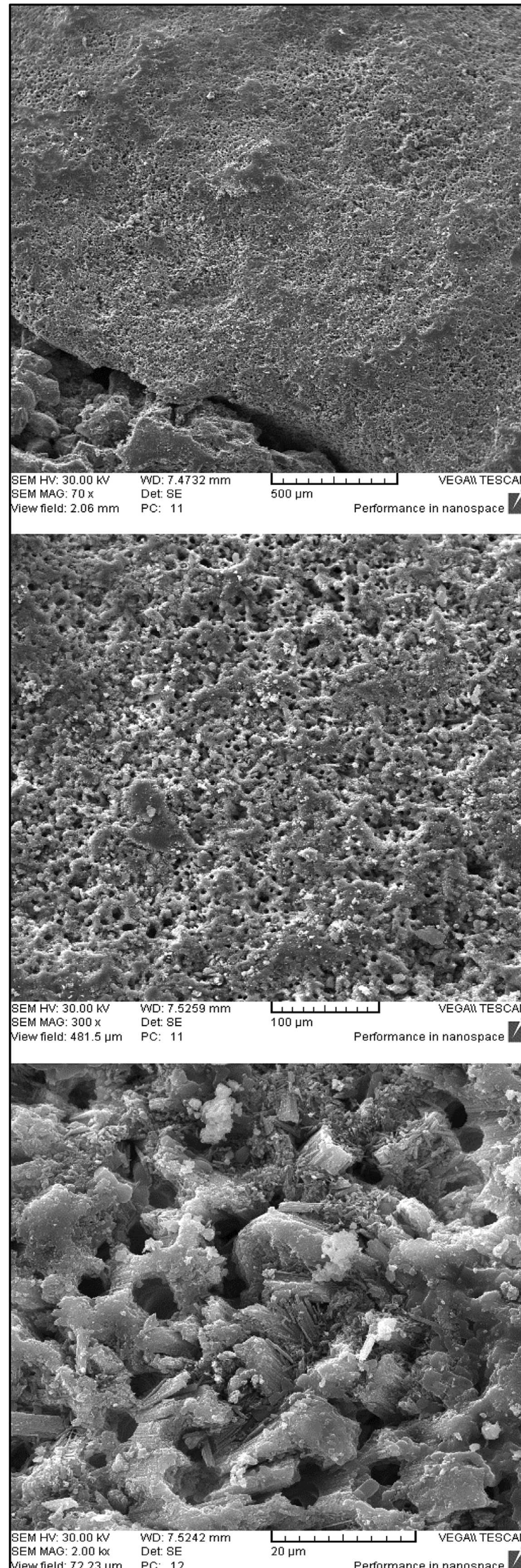

Fig. 1. SEM image of Hormoz carbonate sand with 3 levels of zoom.

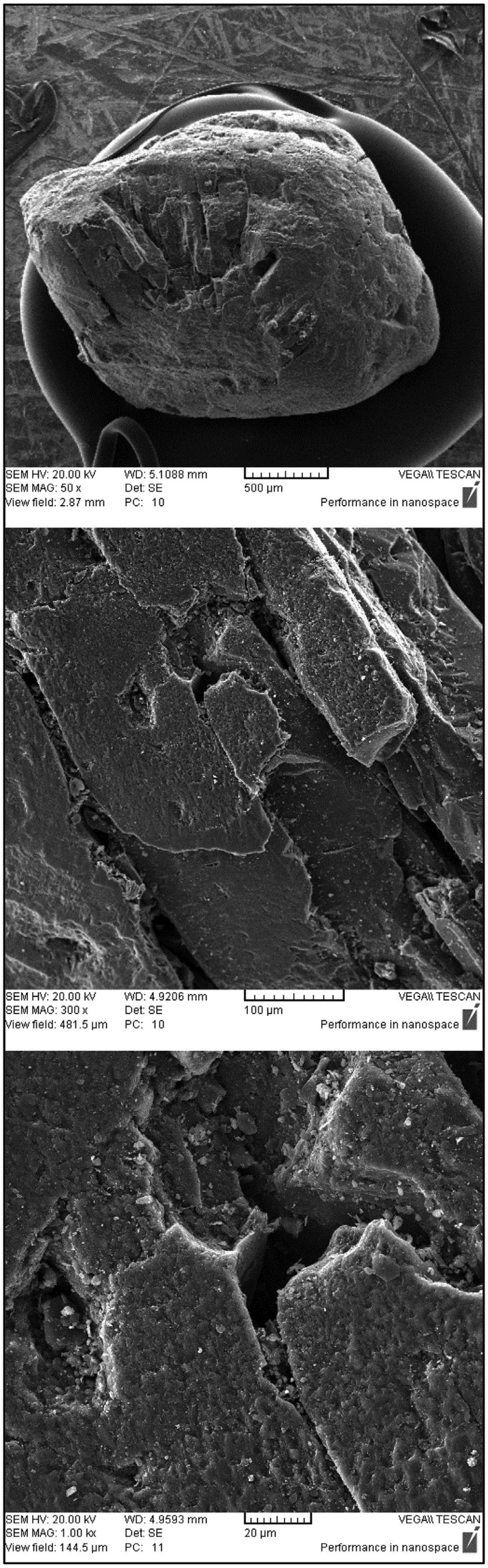

Fig. 2. SEM image of Firuzkuh siliceous sand with 3 levels of zoom.

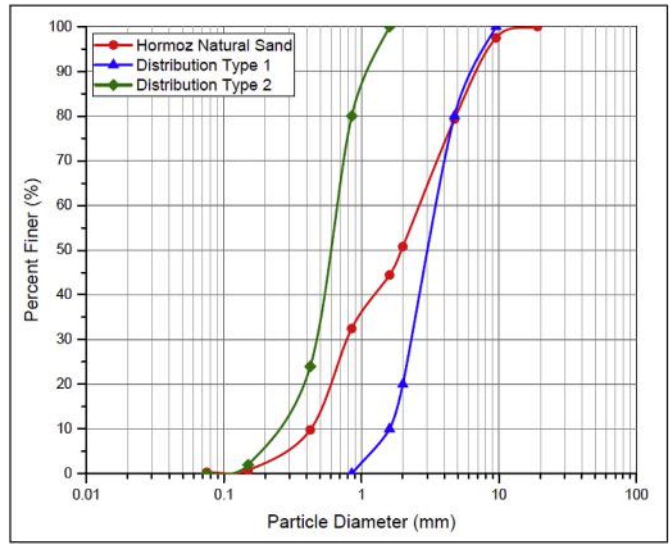

Fig. 3. Particle size distribution curves for natural Hormoz sand and artificial distributions for triaxial tests.

this soil (Hassanlourad et al., 2010). Siliceous sand was obtained from Firuzkuh in the north of Iran. Azizkandi et al. (2014, 2018) reported the specification of Firouzkhoh sand under dynamic and static loading. The Scanning Electron Microscope (SEM) photographs of carbonate and siliceous sand are shown in Fig. 1 and Fig. 2, respectively. Each figure presents three levels of zoom, and a comparison of the two figures indicates that carbonate sand has high intraparticle void space (within the particles), which plays a key role in the behavior of these sediments. The particle form analysis demonstrates that the percentage of platy and rod shaped particles of carbonate sediment is much higher than siliceous sand. The surfaces of carbonate particles are very rough, which increases the friction between particles. The irregularity in shapes and the roughness of carbonate particles lead to an increase in the shear strength of sand.

Particle size distributions of specimens are shown in Fig. 3. Two different particle size distributions were utilized to investigate the effect of particle size on the mechanical behavior of carbonate samples, whereas for siliceous sand only type 2 distribution (see Fig. 3) was used. The sand properties are presented in Table 1.

2.2. Geotextile

This research utilized three types of nonwoven geotextiles with a different mass per unit areas and tensile strengths to investigate the effect of geotextile types on the strength of samples. Nonwoven geotextiles are usually divided into different groups based on their mass per unit areas. This parameter represents the amount of material used in geotextile, the price range, and the tensile strength (an increase in the mass per unit area increases both the tensile strength and price of the geotextile). Table 2 presents the physical and mechanical properties of the geotextile as obtained from the data sheets, which were provided by producer company.

3. Sample preparation and testing procedure

To investigate the effect of geotextile inclusion on the mechanical behavior of carbonate and siliceous sand, a series of drained triaxial compression tests were conducted on the reinforced and unreinforced sand. All test specimens were 70 mm in diameter and 140 mm high. The parameters evaluated in this research are given as follows:

- The number of layers and geotextile arrangement (shown in Fig. 4)

Table 1
Physical and mechanical properties of Carbonate and siliceous sand.

	Sand Type	$\gamma_{d\ min}$ (kN/m^3)	$\gamma_{d\ max}$ (kN/m^3)	D_{10} (mm)	D_{30} (mm)	D_{60} (mm)	C_u	C_c	Unified Soil Classification
Distribution type 1	Carbonate	11.59	13.52	1.6	2.12	3.3	2.06	0.85	SP
Distribution type 2	Carbonate	15.32	17.59	0.25	0.47	0.66	2.64	1.34	SP
Distribution type 2	Siliceous	14.21	16.61	0.25	0.47	0.66	2.64	1.34	SP

Table 2
Physical and mechanical properties of geotextile.

	Mass per unit area (g/m^2)	Thickness (mm)	Ultimate tensile strength (kg/m)	Axial strain at failure (%)
Geotextile type 1	200	1.83	427.86	101.98
Geotextile type 2	400	3.47	697.6	106.97
Geotextile type 3	550	4.04	770.64	75.31

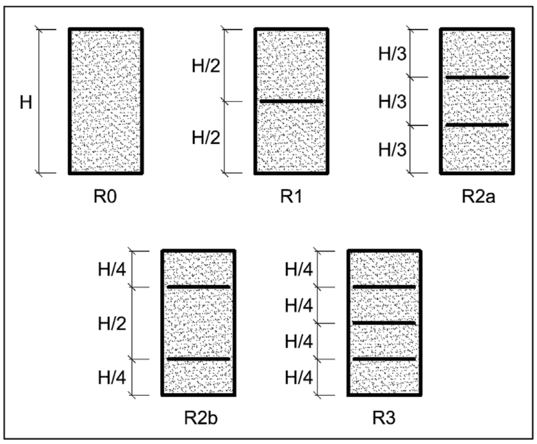

Fig. 4. Geotextile arrangements for triaxial compression tests.

- Particle size (presented in Fig. 3)
- Confining pressure (150, 300, and 450 kPa)
- The relative density of samples (45%, 70%, and 94%)
- Geotextile type (200, 400, and 550 g per square meter)

The number of sand layers in the specimen was chosen based on the geotextile arrangement (6 or 8 layers); the sand was then poured into a mold using a long funnel. Carbonate sand for specimens with 45% relative density was poured into the mold from a constant distance. For specimens with 70% relative density, the mold was vibrated during the process of pouring sand to achieve the desired density, and for specimens with 94% relative density in addition to vibrating the mold, sand layers were compacted by a tamper. It should be noted that in this research, relative density was considered after consolidation. After pouring each sand layer, the distance from the soil surface to the mold top was measured by a caliper, and the density was checked to ensure that the specimen was constructed according to the specifications. Geotextiles were cut with a diameter which was slightly less than the sample diameter and were placed horizontally in the specimen at a specific height based on the arrangement. The saturation of specimens is an important step in the triaxial test because the volumetric strain fluctuation influences the calculated parameters, namely the experimental results. To achieve full saturation, carbon dioxide gas was circulated into the specimen for 20–30 min to replace the air. It is notable that CO_2 dissolves in water easier than the other gases and helps in achieving full saturation (Jafarian et al., 2018b). In addition to circulating CO_2, water was de-aired in a cylinder by a vacuum pump and then was circulated through the specimen. The quality of saturation was specified by the Skempton pore pressure coefficient B; the specimen was considered saturated if B was greater than 0.95. After saturation, samples were consolidated with three confining pressures (150, 300, and 450 kPa). All the consolidated drained triaxial tests were conducted according to ASTM D7181 using a strain rate of 0.5 mm per minute, and the tests were continued up to an axial strain of 20%.

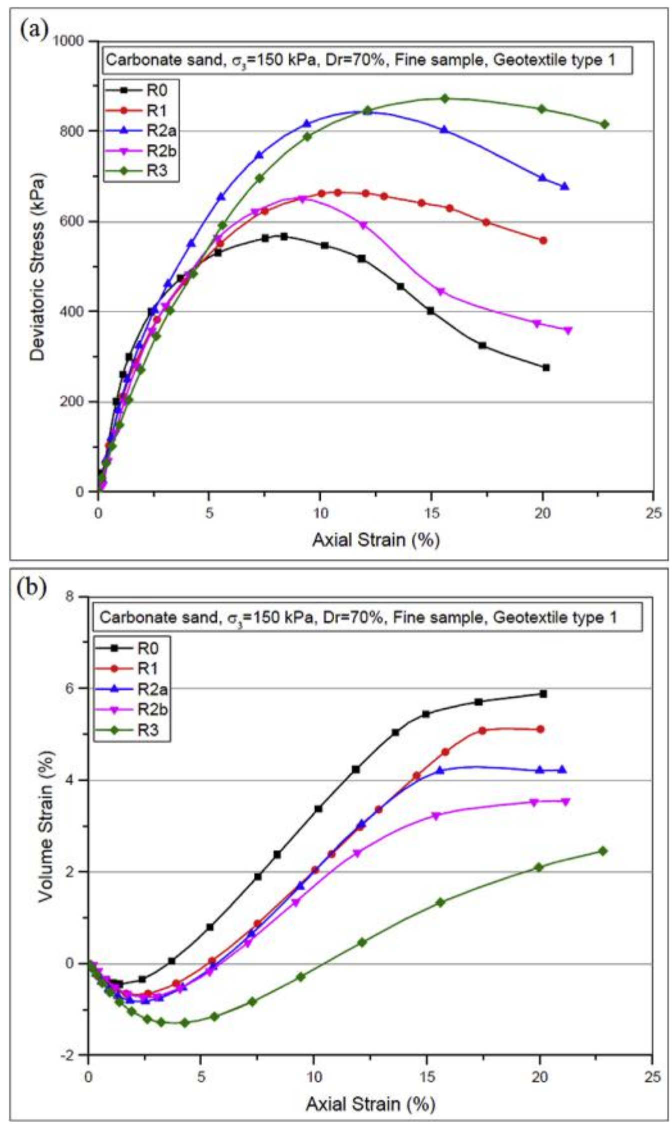

Fig. 5. Effect of geotextile arrangement on fine carbonate specimens with 70% relative density and geotextile type 1 under 150 kPa confining pressure. (a) Deviatoric Stress-Axial Strain curves (b) Volumetric-Axial Strain curves.

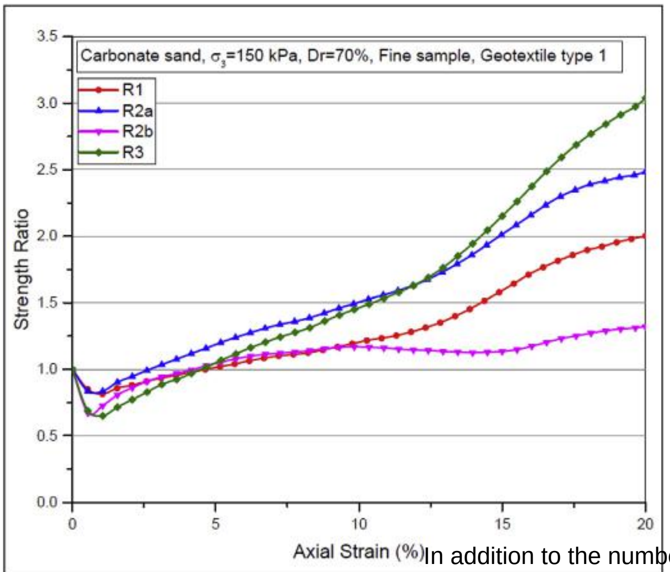

In addition to the number of geotextile layers, the arrangement of the layers in soil is also important

Fig. 6. Effect of geotextile arrangement on normalized curves for fine carbonate sand with 70% relative density and geotextile type 1 under 150 kPa confining pressure.

4. Test results

4.1. Effect of the number of geotextile layers and their arrangement

One of the most significant parameters for designing reinforced soil is reinforcement arrangement, which is defined by vertical distances between layers (Hong and Wu, 2013; Sommers and Viswanadham, 2009; Xu and Fatahi, 2018). Decreasing the vertical distance of layers increases the overall costs of projects. Therefore, choosing the optimized number and arrangement of geotextile is vital. Four arrangements were utilized in this study to investigate the effect of geotextile arrangement on the mechanical behavior of reinforced carbonate sand. Results of consolidated drained triaxial tests for specimens with 70% relative density under 150 kPa confining pressure are shown in Fig. 5.

As illustrated in Fig. 5 reinforcing carbonate sand with geotextile significantly increases the peak strength and axial strain at failure, and the enhancement becomes more noticeable with an increase in the number of geotextile layers. In addition to the number of geotextile layers, the arrangement of the layers in soil is also important. Both R2a and R2b arrangements use two layers of geotextile to reinforce specimens. However, the strength enhancement is far better when the reinforcement layers have an equal distance (R2a) than in cases where the reinforcements are placed near the top and bottom of the specimens (R2b). This behavior is attributed to the fact that the maximum radial strain in triaxial tests occurs in the middle of specimens, and its quantity decreases with approaching to caps of the samples; thus, the radial strain at the reinforcement position in R2a, which reinforcements are closer to the middle of specimens, is higher than R2b. Consequently, the tensile force in reinforcement and the strength enhancement is more in R2a than R2b arrangement. This finding indicates that in optimized reinforced soil design, reinforcements should be placed in sections that are predicted to have higher displacements. Application of geotextile reduces the loss of post-peak strength; in some specimens reinforced with three layers of geotextile, no post-peak loss of shear strength is observed.

Volumetric-Axial strain curves of unreinforced and reinforced carbonate sand under 150 kPa confining pressure are shown in Fig. 5 (b). It should be noted that the positive and negative values of volumetric strain represent dilative and contractive behavior respectively. The unreinforced sample exhibits contractive behavior at low axial strains; however, the behavior reverses from contractive to dilative at higher axial strains, which is consistent with the observation reported by other researchers. (Hyodo et al., 1996; LaVielle, 2008; Salem et al., 2013). Reinforced samples exhibit more contractive behavior than the unreinforced specimen. This behavior is attributed to the compressibility of geotextile layers. In fact, the thickness of geotextile layers decreases due to initial axial strain; hence, reinforced specimens exhibit more contractive behavior at the low axial strains. With the growth of axial strain and reversing the specimen behavior from contractive to dilative, geotextile layers restrain the lateral deformation resulting in a reduction of volumetric strain of samples at high axial strains.

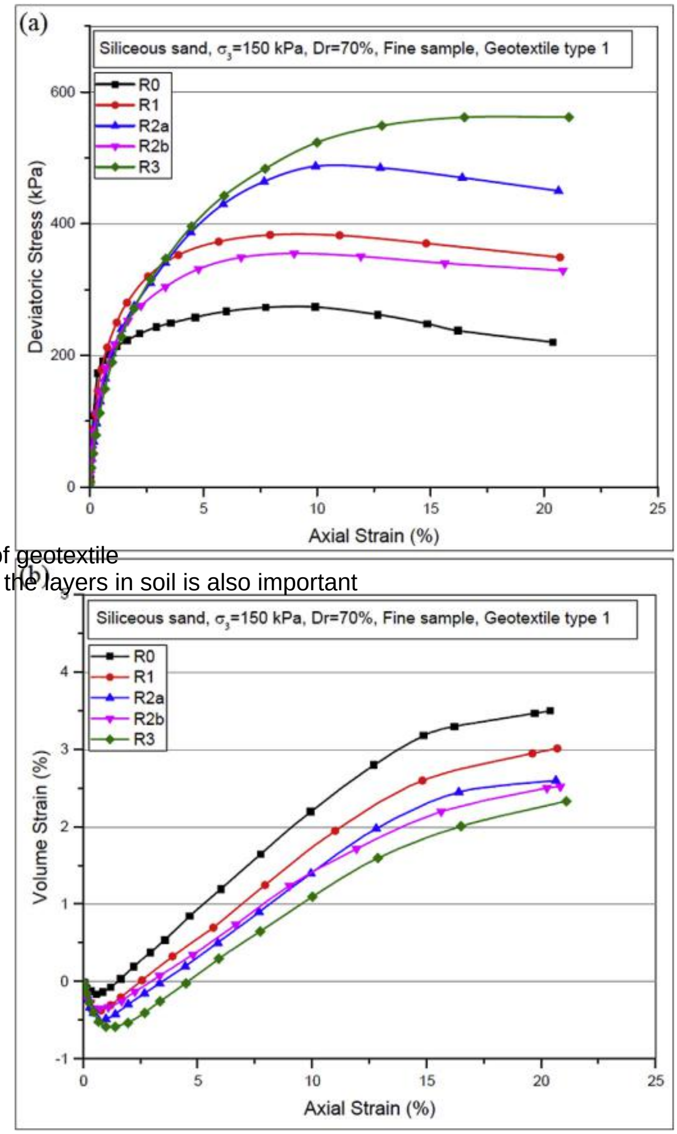

Fig. 7. Effect of geotextile arrangement on fine siliceous specimens with 70% relative density under 150 kPa confining pressure. (a) Deviatoric Stress-Axial Strain curves (b) Volumetric-Axial Strain curves.

Normalized strength ratio-axial strain curves are employed in this research to determine the amount of strength enhancement in reinforced specimens. Strength ratio is defined as the proportion of deviatoric stress in reinforced specimens to unreinforced ones in a specific strain. Fig. 6 shows a normalized curve of fine sand under 150 kPa confining pressure.

As illustrated in Fig. 6 the strength ratio of reinforced specimens at axial strains less than 4–5% is lower than one. This denotes that at low strains, the shear strength of reinforced samples is less than that of

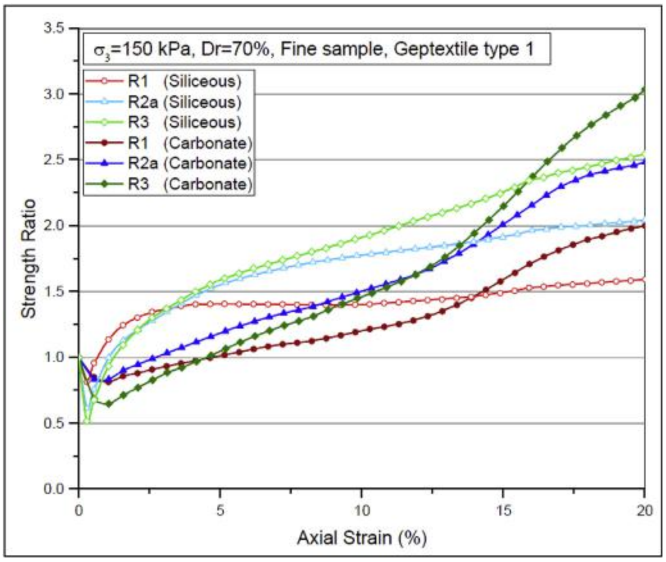

Fig. 8. Effect of sand type on normalized strength ratio-axial strain curves for fine specimens with 70% relative density under 150 kPa confining pressure.

unreinforced samples. This behavior is attributed to the fact that to enhance the strength in reinforced samples, the geotextile should deform to mobilize its tensile force. In other words, while the mobilized tensile force in geotextile is not sufficient to increase the shear strength of specimens at axial strains of less than 5%, increasing the axial strain and mobilizing the tensile force in the geotextile increases the strength ratio. This behavior is consistent with the results reported by Nguyen et al. (2013). It should be noted that in the actual construction site, a high percentage of the required geotextile deformation for enhancing the shear strength occurs during GRS construction, which is due to a surcharge load of soil (Nicks et al., 2016). Thus, the decision of utilizing geotextile reinforcement in carbonate sand depends on the type of geotechnical project in terms of strain limitation and strain occurrence during construction. The application of geotextile reinforcement can be very beneficial in many projects such as the stabilizing of a steep slope, in which the total stability of slope takes precedence over its deformation.

As shown in Fig. 6 the strength ratio for three layers of geotextile under 150 kPa confining pressure reaches to 3.01 at high axial strains. Strength ratio of R2b arrangement with two layers of geotextile is less than R1 arrangement with one layer of geotextile in the middle of specimens. This outcome indicates the significance of placing reinforcement in the section with the maximum displacement.

4.2. Effect of sand type

Triaxial tests were performed on carbonate and siliceous sand to compare the effect of geotextile reinforcement on the mechanical behavior of these types of sand. Results of triaxial tests for siliceous specimens with 70% relative density under 150 kPa confining pressure are shown in Fig. 7. The inclusion of geotextile reinforcement increases the shear strength of siliceous samples, which is similar to that of carbonate specimens. However, as illustrated in Fig. 5, the loss of post-peak strength in unreinforced carbonate sand is much higher than siliceous sand. The crushing of carbonate sand, which results in augmentation of volumetric compression, and particles' angular shapes may account for the high loss of post-peak strength in carbonate sand. Thus, reinforcing carbonate sand with geotextile is more efficient than siliceous sand because geotextile reinforcement mitigates the loss of post-peak strength significantly. A comparison of Figs. 7 (b) and Fig. 5 (b) highlights that carbonate samples exhibit more contractive behavior than siliceous specimens at low axial strains since carbonate sands have

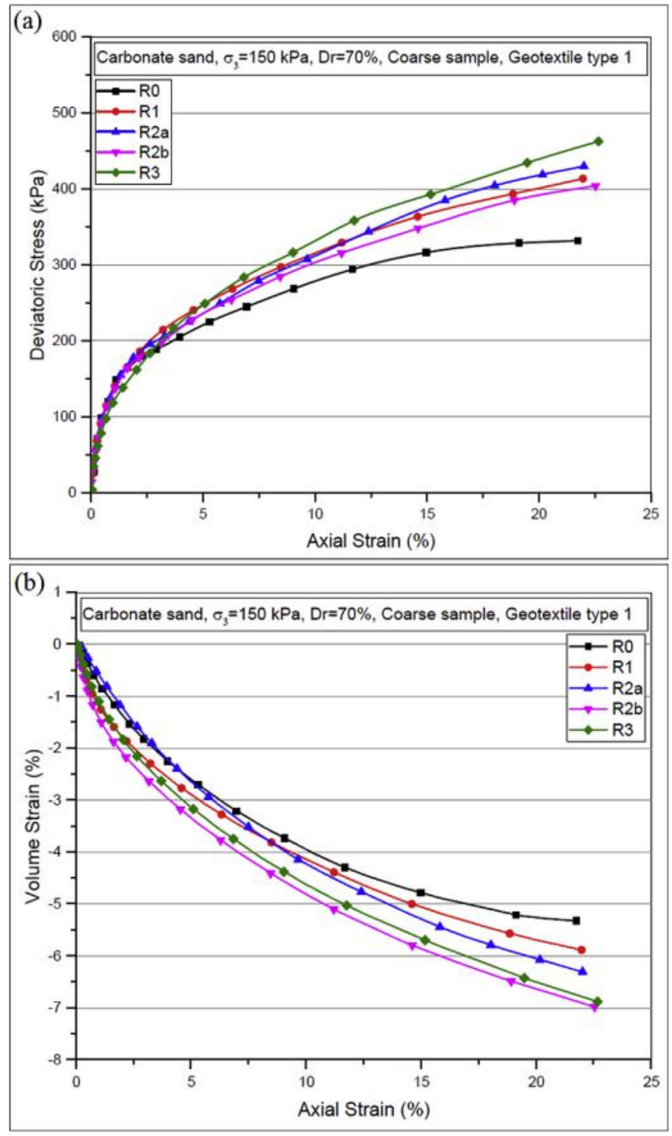

Fig. 9. Effect of geotextile arrangement on coarse specimens with 70% relative density and geotextile type 1 under 150 kPa confining pressure. (a) stress-axial strain curves (b) volumetric-axial strain curves.

higher void ratio than siliceous sands as a result of their irregular particles' shapes (Arango, 2006). Shearing samples disrupt the soil structures, and soil particles tend to rearrange to a denser state of packing, which leads to contractive behavior and a decrease in the void ratio of samples. The process of rearranging carbonate particles takes longer than siliceous sands due to the inherent high void ratio of carbonate sands. Therefore, reinforced and unreinforced carbonate specimens exhibit more contractive behavior than their corresponding siliceous samples and tend to dilate at higher axial strains. This result is consistent with the observation stated by Shahnazari et al. (2014).

Normalized curves of strength ratio-axial strain for siliceous and carbonate specimens are shown in Fig. 8. Axial strains at the strength ratio equal to one are lower in siliceous samples than carbonate specimens. In other words, the range of axial strain in siliceous samples (in which the strength of reinforced samples is less than the unreinforced specimen) is limited to 2%, which is lower than that of carbonate specimens. As earlier explained, this behavior is attributed to the fact that dilation in siliceous sand occurs earlier than carbonate samples. Consequently, in cases where the axial strain is lower than 5%, the greater dilation in siliceous samples leads to the higher radial strain.

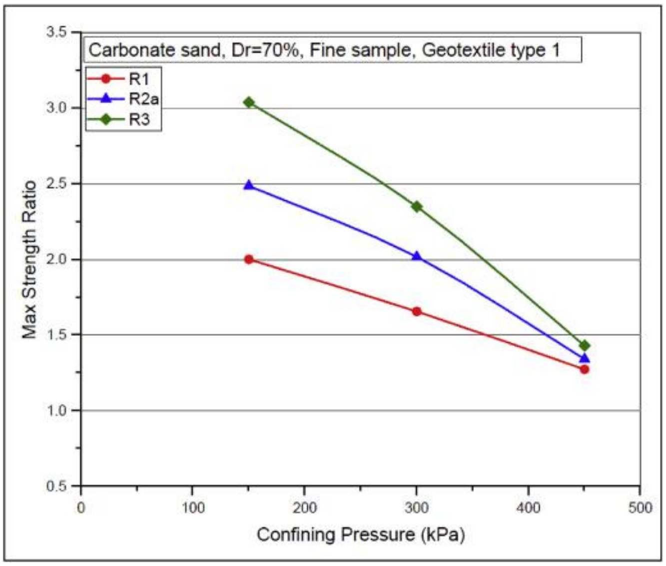

Fig. 10. Maximum strength ratio-confining pressure for fine specimen with 70% relative density and geotextile type 1.

Thus, the radial strain needed to mobilize the geotextile tensile force for increasing the samples' strength occurs at lower axial strains in siliceous sand. The strength ratio of carbonate specimens at axial strains greater than 15% is higher than siliceous samples.

4.3. Effect of particle size

Two particle size distributions were utilized in this research to evaluate the effect of particle size on the strength enhancement of carbonate reinforced sand. Results of triaxial tests for coarse specimens with 70% relative density under 150 kPa confining pressure are shown in Fig. 9.

A comparison of Fig. 5 and Fig. 9 which illustrate results of fine and coarse carbonate sand respectively with other identical conditions indicates that fine carbonate sand reinforcement is much more productive than coarse sand reinforcement. This may be partly due to the fact that increasing the particle size in Hormoz carbonate sands changes the shapes of many particles from spherical to planar form (Fatemiaghda et al., 2017). Due to compaction of samples, planar particles are usually placed in a parallel direction with geotextile layers and produce very low friction in the geotextile-sand interface. Thus, the interlocking of geotextile layers with fine and spherical carbonate sand is much better than coarse and planar particle sand which results in the higher strength enhancement of fine samples. After test completion, the geotextile layers were retrieved from the dismantled specimens; a caliper was used to measure diameters of the reinforcements both before and after the tests in 3 different directions and their strains were calculated. The strains of geotextile layers retrieved from fine specimens were six times more than the ones retrieved from coarse samples. This finding indicates that the interlocking of geotextile with coarse and planar carbonate sand was not sufficient to deform geotextile layers and mobilize their tensile force. The other reason for low strength enhancement in coarse samples is due to the fact that the radial strain of dilated samples increases more than contracted specimens. As illustrated in Fig. 9 (b), no dilation occurs in the coarse samples; thus, the radial strain of these samples and as a result, their strength enhancements are less than the corresponding fine samples.

4.4. Effect of confining pressure

Confining pressure in triaxial tests simulates the surrounding soil pressure on the specimens. To investigate the effect of confining pressure on the strength of reinforced carbonate sand, three confining pressures of 150, 300, and 450 kPa were used in the present study. Fig. 10 shows maximum strength ratio-confining pressure curves for three arrangements.

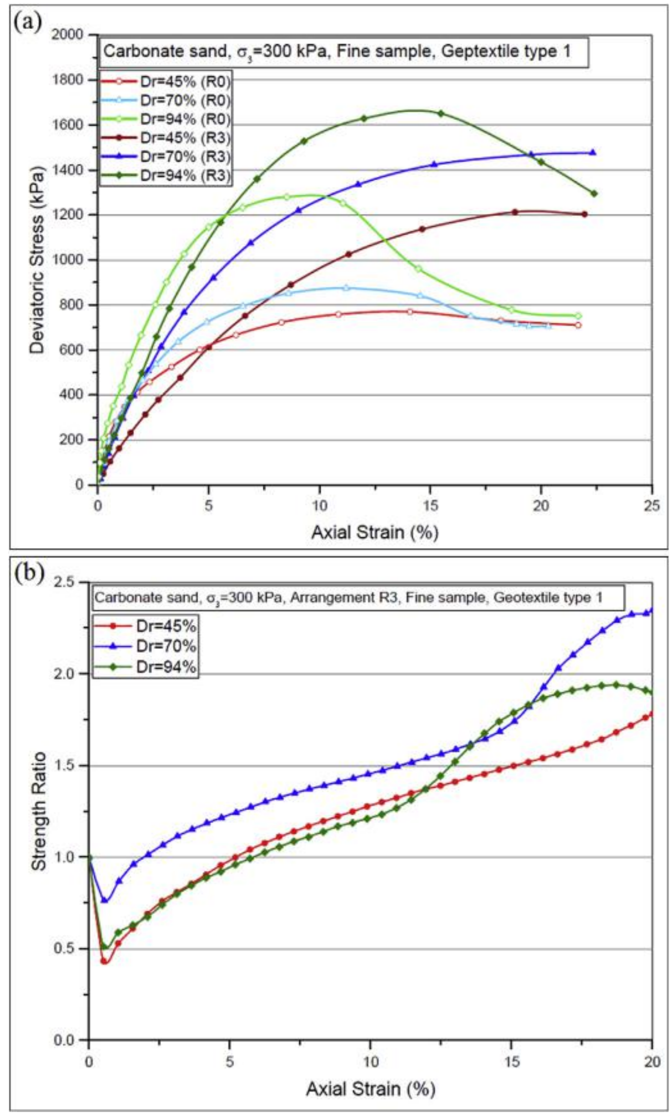

Fig. 11. Effect of relative density on fine specimens reinforced with geotextile type 1 and R3 arrangement under 300 kPa confining pressure (a) stress-axial strain curve (b) strength ratio-axial strain curve.

As can be seen in Fig. 10, increasing confining pressure decreases the strength ratio of reinforced sand. This finding indicates that in soil of great depth, in which confining pressure is high, reinforcing soil with geotextile has low efficiency and increases the shear strength slightly. However, the shear strength is significantly enhanced in soil of low depth, in which confining pressure is low. In fact, reinforcing sand with geotextile layers decreases the dilative behavior of sand and has a confining effect on specimens. In high confining pressures, the inclusion of geotextile has a low confining effect on specimens, which leads to an insignificant augmentation of shear strength. It is observed that in 450 kPa confining pressure, the strength ratio of one, two and three layers of geotextile have minor differences with each other.

4.5. Effect of relative density

Three relative densities (i.e. 45%, 70%, and 94%) were used in this research. In sand specimens, a higher relative density leads to higher

Fig. 12. Image of ruptured geotextile type 1 after experiment of samples with 94% relative density.

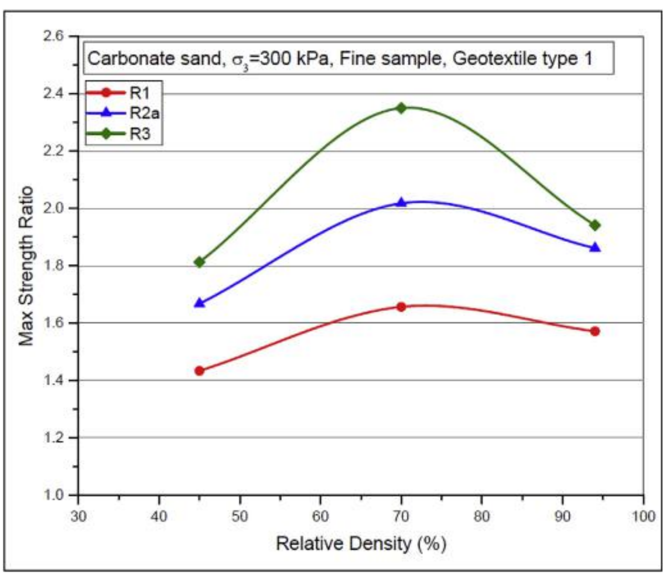

Fig. 13. Maximum strength ratio-relative density curves for fine specimens with geotextile type 1 under 300 kPa confining pressure.

dilation which facilitates mobilization of reinforcement elements inside the samples (Tizpa et al., 2015). It should be noted that relative density was considered after consolidation. Fig. 11 shows the effect of relative density on fine carbonate sand specimens.

As illustrated in Fig. 11 (a), an increase in the relative density increases the maximum shear strength of specimens, but a significant post-peak loss of shear strength is observed in the reinforced sample with 94% relative density. Post-peak loss of strength is not, however, detected in the other reinforced specimen with 70% relative density, which proves that geotextile inclusion considerably reduces the post-peak loss of strength. However, the reduction of post-peak strength loss is not observed in the reinforced specimen with 94% relative density which is due to the rupture of geotextile layers. In fact, in these specimens, the geotextile layers interrupting the shear plane were ruptured during loading and lost their efficiency (Fig. 12). The measured geotextile strain after tests completion for specimens with 45% and 70% relative densities were 4.2 and 5.4 percent, respectively.

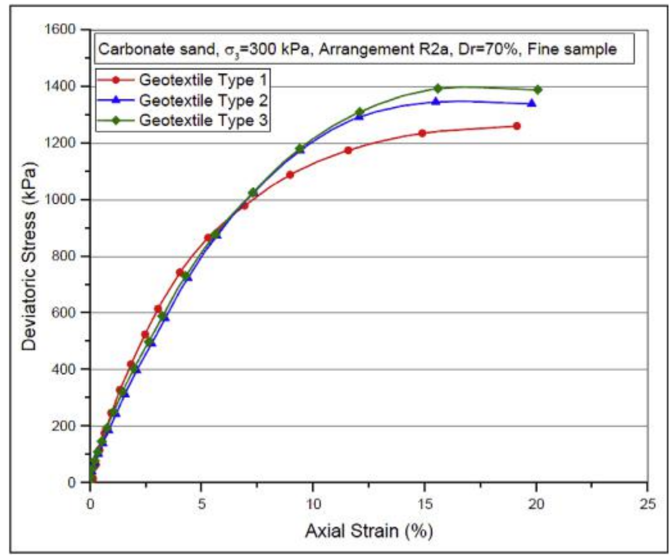

Fig. 14. Effect of geotextile type on fine specimen with 70% relative density and R2a arrangement under 300 kPa confining pressure.

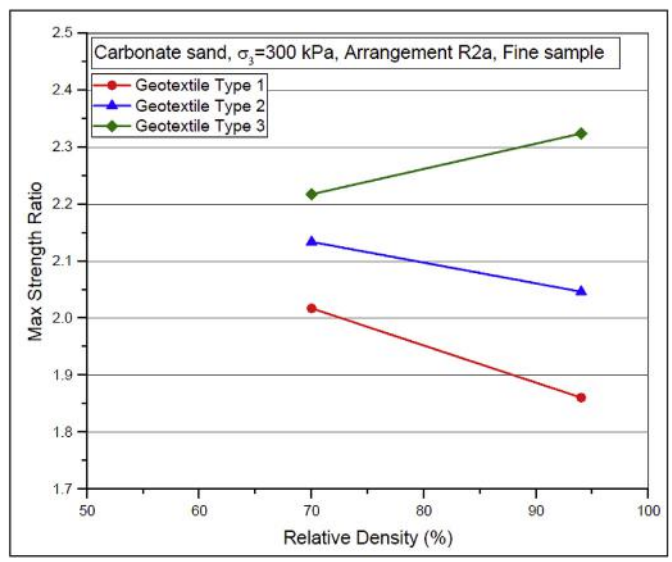

Fig. 15. Maximum strength ratio-relative density for fine specimens with R2a arrangement under 300 kPa confining pressure.

As can be observed in Fig. 11 (b), increasing the relative density from 45% to 70% increases the strength ratio. Increasing the relative density also increases particle contact with each other and with geotextile layers as well. Consequently, the interlocking of geotextile-carbonate sand interface rises. The strength ratio, therefore, increases with increasing the relative density from 45% to 70%. However, increasing the relative density of specimens from 70% to 94% not only failed to enhance the strength ratio, but also decreased it. In specimens with 94% relative density, the interlocking of carbonate sand with layers of geotextile was extremely high. Thus, the incoming tensile force from carbonate sand was more than the ultimate tensile strength of geotextile and ruptured them. Fig. 13 shows maximum strength ratio-relative density curves for three arrangements.

4.6. Effect of geotextile type

Geotextile property plays an important role in the mechanical

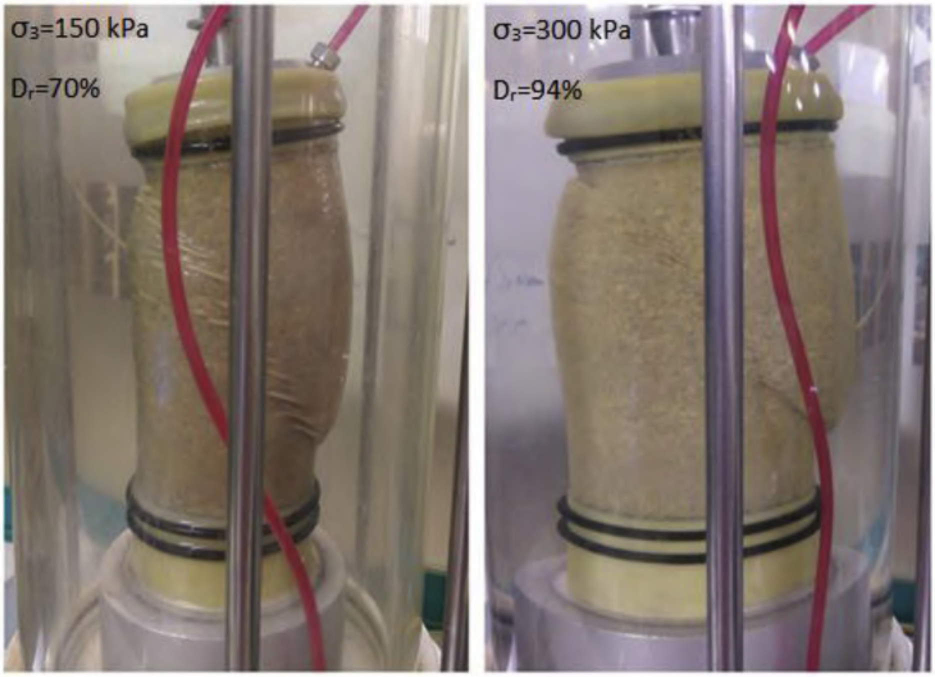

Fig. 16. Images of failed unreinforced specimens.

behavior of reinforced soil (Chen et al., 2018; Markou, 2016; Sayeed et al., 2014). In this research, the geotextile type specifies the mass per unit area of nonwoven geotextiles. The mass per unit area of geotextile represents the material used to produce them; with an increase in the mass per unit area of geotextile, their price and ultimate tensile strength increases. Thus, for an optimized design, geotextile with a specific mass per unit area should be selected which has the highest strength enhancement with respect to its price. In this research, geotextiles with 200, 400, and 550 g/m^2 were used to evaluate the effect of geotextile type on the strength enhancement of carbonate sand. Fig. 14 shows stress-axial strain and strength ratio-axial strain curves for R2a arrangement under 300 kPa confining pressure.

As illustrated in Fig. 14, with an increase in the mass per unit area of geotextiles, the maximum deviatoric stress increases. However, the amount of strength enhancement with respect to the price of a geotextile with a higher mass per unit area is insignificant. As can be seen in Fig. 14 the maximum deviatoric stress for geotextile type 1 with 200 g/m^2 is 1263 kPa. Despite doubling the mass per unit area in geotextile type 2, the deviatoric stress increased by only 84 kPa and reached 1347 kPa. While the mass per unit area of geotextile type 3 is 2.75 times more than geotextile type 1, the deviatoric stress increased by only 134 kPa and reached 1397 kPa. It can thus be concluded that increasing the mass per unit area of geotextiles for further strength enhancement is not economical.

As earlier discussed in section 4.5, the strength ratio of specimens reinforced with geotextile type 1 and 70% relative density was higher than 94% relative density since geotextile type 1 ruptured due to high tensile force. In this part, specimens were reinforced with other mass per unit area geotextiles to evaluate the effect of geotextile type on specimens with the high relative density (Fig. 15). Results indicate that geotextile type 2 was ruptured, and the strength ratio decreased by increasing the relative density from 70% to 94%. However, geotextile type 3 did not rupture even in the high relative density; consequently, the strength ratio increased by increasing the relative density from 70% to 94%. As a rule, the strength ratio of reinforced samples increases with increasing the relative density as long as the geotextile does not rupture.

4.7. Effect on failure pattern

Dense specimens in triaxial tests exhibit the maximum shear strength and post-peak loss of strength (Benessalah et al., 2016; Haeri et al., 2000; Nguyen et al., 2013). The failure pattern of these samples is along a shear plane close to the angle of $45 + \varphi/2$. The images of unreinforced samples that failed along a shear plane are shown in Fig. 16. Geotextile inclusion limits the lateral expansion of specimens during loading. Consequently, the failure pattern changes from a shear plane to bulging between adjacent layers of geotextile. The bulging failure pattern of reinforced carbonate specimens are displayed in Fig. 17.

Fig. 18 shows the images of failed reinforced samples with 94% relative density. As discussed in section 4.5, geotextiles ruptured under this relative density due to high interlocking between sand particles and geotextile layers. As illustrated in Fig. 18 ruptured geotextiles could not limit the lateral expansion of specimens, and the bulging failure pattern was not observed in these specimens.

5. Conclusions

In this research, a series of consolidated drained triaxial tests were conducted on reinforced carbonate and siliceous specimens to compare their reinforced behavior and evaluate parameters that affect the mechanical behavior of reinforced carbonate sand. The parameters investigated in this paper are the number of geotextile layers, their arrangement in specimens, confining pressure, and the relative density of samples. In order to study the effect of carbonate particle size and geotextile type, two particle size distributions and three types of nonwoven geotextiles with different mass per unit areas were utilized in this study. The conclusions are summarized as follows:

1. Geotextile reinforcement significantly reduces the post-peak strength loss of carbonate specimens and increases the peak strength and axial strain at failure. The strength enhancement is improved by increasing the geotextile layers.
2. The peak strength of the R2b arrangement with two geotextile layers is lower than the R1 arrangement with one geotextile layer. This finding indicates that in addition to the number of geotextile

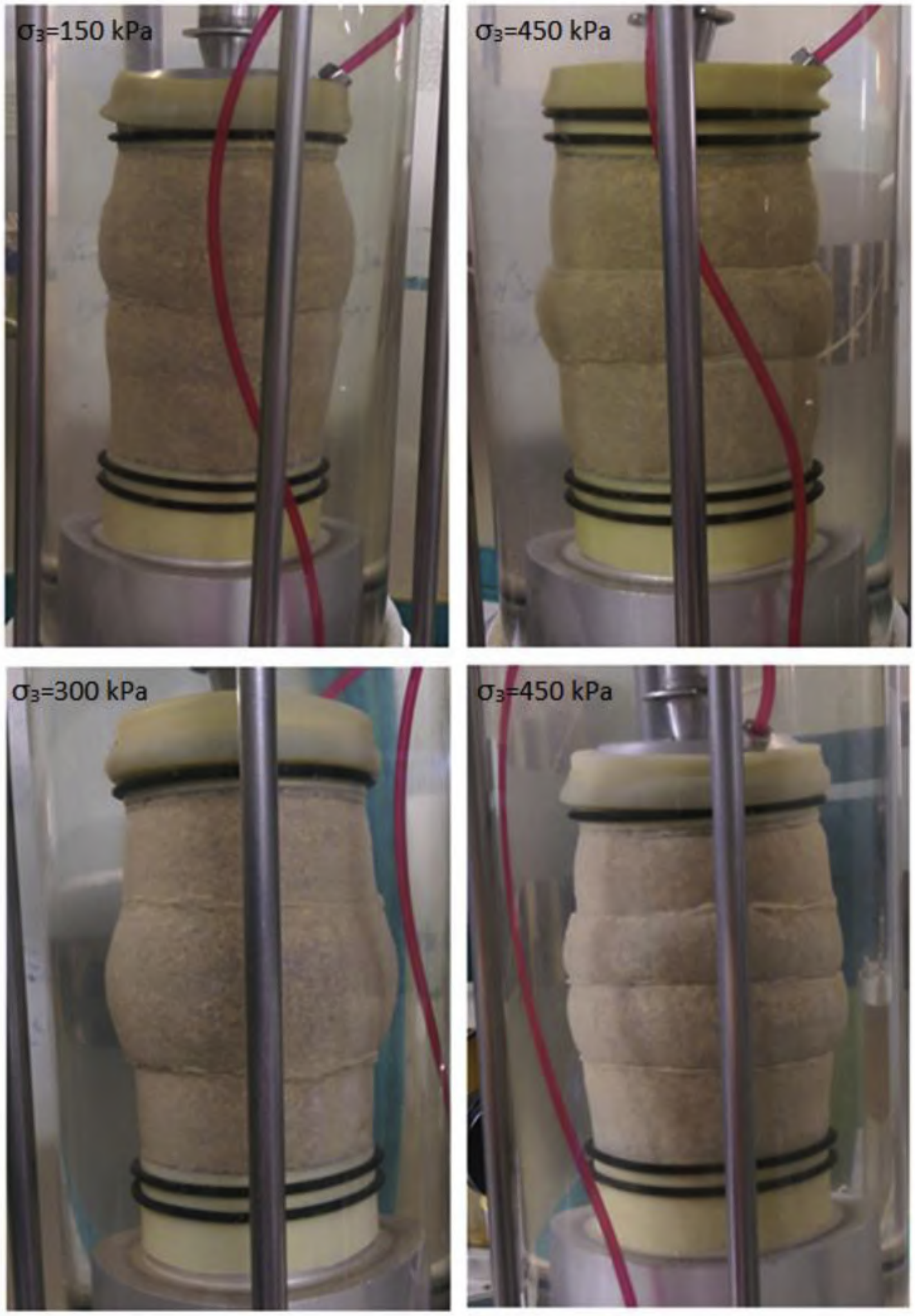

Fig. 17. Bulging failure pattern of reinforced specimens with 70% relative density.

layers, their arrangement in specimens also affects the behavior of reinforced sand. In order to achieve better strength enhancement, geotextile layers should be placed in specific sections of samples that possess higher radial strain.

3. The strength ratio of reinforced carbonate sand under axial strains less than 4–5% is lower than one since the radial strain and as a result, the reinforcement deformation is not sufficient to mobilize the tensile force in geotextile layers. It should be noted that in the actual construction site, a high percentage of this required deformation occurs during construction; hence, the decision of utilizing geotextile reinforcement in carbonate sand depends on the type of project in terms of strain limitation and strain occurrence during construction.
4. At low axial strains, reinforced carbonate sand exhibit more contractive behavior than the unreinforced sample due to the compressibility of geotextile layers. At high axial strains, geotextile layers restrain the lateral deformation of samples and reduce the volumetric strain.
5. While the inclusion of geotextile in siliceous samples is similar to carbonate specimens in terms of increasing the shear strength, the strength ratio of a siliceous specimen is lower than the corresponding carbonate sample at high axial strains.
6. The loss of post-peak strength in carbonate unreinforced sand is much higher than siliceous sand, which is probably due to the crushing of carbonate particles and their angular shapes. Thus, reinforcing carbonate sand with geotextile is more beneficial than siliceous sand with regard to the high reduction of post-peak strength loss in reinforced specimens.

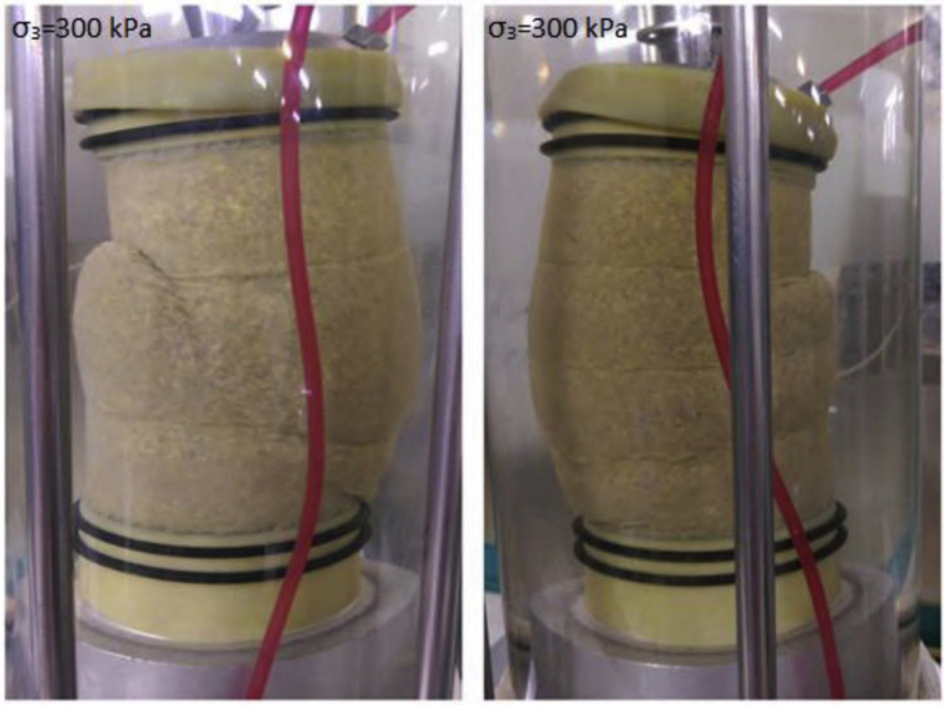

Fig. 18. Failure pattern of specimens with 94% relative density that were reinforced with geotextile type 1 and 2.

7. Reinforced and unreinforced carbonate specimens exhibit more contractive behavior than their corresponding siliceous samples and tend to dilate at higher axial strains due to their inherent high void ratio.
8. The axial strain range with a strength ratio of less than one is limited to 2% in siliceous samples, which is lower than carbonate samples. This behavior is attributed to the fact that the dilation of siliceous samples occurs at lower axial strains and provides the deformation needed for mobilizing the geotextile tensile force.
9. Reinforcing fine carbonate sand with geotextile leads to more strength enhancement than coarse sand since a high percentage of coarse carbonate particles are planar; moreover, dilation does not occur in coarse samples to further increase the radial strain, which is required for the strength enhancement of samples.
10. In both carbonate and siliceous specimens, the strength ratio decreases as confining pressure increases.
11. The strength ratio improves as the relative density increases, which is due to the increase of interlocking between geotextile layers and carbonate particle. This process continues as long as the geotextile does not rupture.
12. Utilizing geotextile with higher mass per unit areas for further strength enhancement is uneconomical since the amounts of strength augmentation for various types of geotextiles vary slightly.
13. The failure pattern in unreinforced specimens is along a shear plane, but geotextile limits the lateral expansion and changes the failure pattern to bulging between adjacent layers.

Nomenclature

D_r	relative density after consolidation
σ_3	confining pressure
C_u	coefficient of uniformity
C_c	coefficient of curvature
$\gamma_{d\ max}$	maximum dry density
$\gamma_{d\ min}$	minimum dry density
D_{10}	grain diameter at 10% passing
D_{30}	grain diameter at 30% passing
D_{60}	grain diameter at 60% passing
SP	poorly graded soil
B	Skempton's saturation parameter
CD	consolidated drained triaxial test

References

Afzali-Nejad, A., Lashkari, A., Shourijeh, P.T., 2017. Influence of particle shape on the shear strength and dilation of sand-woven geotextile interfaces. Geotext. Geomembranes 45, 54–66. https://doi.org/10.1016/j.geotexmem.2016.07.005.

Arango, C., 2006. Stress strain behavior and dynamic properties of Cabo Rojo calcareous sands. In: Masters Abstracts International.

Azizkandi, A.S., Baziar, M., Modarresi, M., Salehzadeh, H., Rasouli, H., 2014. Centrifuge modeling of pile-soil-pile interaction considering relative density and toe condition. Sci. Iran. 1330–1339.

Azizkandi, A.S., Baziar, M.H., Yeznabad, A.F., 2018. 3D Dynamic Finite Element Analyses and 1 g Shaking Table Tests on Seismic Performance of Connected and Nonconnected Piled Raft Foundations. KSCE J. Civ. Eng. 22, 1750–1762.

Benessalah, I., Arab, A., Villard, P., Merabet, K., Bouferra, R., 2016. Shear Strength Response of a Geotextile-Reinforced Chlef Sand: A Laboratory Study. Geotech. Geol. Eng. 34, 1775–1790. https://doi.org/10.1007/s10706-016-9988-7.

Brandes, H.G., 2011. Simple Shear Behavior of Calcareous and Quartz Sands. Geotech. Geol. Eng. 29, 113–126. https://doi.org/10.1007/s10706-010-9357-x.

Celestino, T.B., Mitchell, J.K., 1983. Behavior of carbonate sands for foundations of offshore structures. Proceedings, Brazil offshore 83, 85–102.

Chen, J.F., Wang, X.T., Xue, J.F., Zeng, Y., Feng, S.Z., 2018. Uniaxial compression behavior of geotextile encased stone columns. Geotext. Geomembranes 46, 277–283. https://doi.org/10.1016/j.geotexmem.2018.01.003.

Chi, P.-C., Fon, K.-Y., Chen, R.-H., 2012. Model tests for anchored geosynthetic slope systems under dry and seepage conditions. Geosynth. Int. 19, 306–318. https://doi.org/10.1680/gein.12.00017.

Coop, M.R., 1990. The mechanics of uncemented carbonate sands. pp. 607–626.

Costa, C.M.L., Zornberg, J.G., Bueno, B. de S., Costa, Y.D.J., 2016. Centrifuge evaluation of the time-dependent behavior of geotextile-reinforced soil walls. Geotext. Geomembranes 44, 188–200. https://doi.org/10.1016/j.geotexmem.2015.09.001.

Datta, M., Gulhati, S., Rao, G.V., 1979. Crushing Of Calcareous Sands During Shear. Soc. Petrol. Eng. J. 20. https://doi.org/10.4043/3525-MS.

Denine, S., Della, N., Muhammed, R.D., Feia, S., Canou, J., Dupla, J.C., 2016. Effect of geotextile reinforcement on shear strength of sandy soil: Laboratory study. Studia Geotechnica Mech. 38, 3–13. https://doi.org/10.1515/sgem-2016-0026.

Fatemiaghda, M., Shahnazari, H., Karami, H.R., Talkhablu, M., 2017. Effect of texture of carbonate soils in South Iran coasts on aggregate crushing. Mar. Georesour. Geotechnol. 35, 986–998. https://doi.org/10.1080/1064119X.2016.1275893.

Golightly, C.R., 1988. Some fundamental properties of carbonate sands, Engineering for Calcareous Sediments. In: Proc. Int. Conf. on Calcareous Sediments, 1988, pp. 69–78.

Gray, D.H., Al-Refeai, T., 1986. Behavior of fabric-versus fiber-reinforced sand. J. Geotech. Eng. 112, 804–820.

Guler, E., Selek, O., 2014. Reduced-Scale Shaking Table Tests on Geosynthetic-Reinforced Soil Walls with Modular Facing. J. Geotech. Geoenviron. Eng. 140, 4014015. https://doi.org/10.1061/(ASCE)GT.1943-5606.0001102.

Haeri, S.M., Noorzad, R., Oskoorouchi, A.M., 2000. Effect of geotextile reinforcement on the mechanical behavior of sand. Geotext. Geomembranes 18, 385–402.

Hassanlourad, M., Salehzadeh, H., Shahnazari, H., 2010. Mechanical properties of ungrouted and grouted carbonate sands. Int. J. Geotech. Eng. 4, 507–516. https://doi.org/10.3328/IJGE.2010.04.04.507-516.

Hong, Y.S., Wu, C. Sen, 2013. The performance of a sand column internally reinforced with horizontal reinforcement layers. Geotext. Geomembranes 41, 36–49. https://doi.org/10.1016/j.geotexmem.2013.10.002.

Hyodo, M., Aramaki, N., Itoh, M., Hyde, A.F.L., 1996. Cyclic strength and deformation of crushable carbonate sand. Soil Dynam. Earthq. Eng. 15, 331–336.

Jafarian, Y., Javdanian, H., Haddad, A., 2018a. Strain-dependent dynamic properties of Bushehr siliceous-carbonate sand: Experimental and comparative study. Soil Dynam. Earthq. Eng. 107, 339–349. https://doi.org/10.1016/j.soildyn.2018.01.033.

Jafarian, Y., Javdanian, H., Haddad, A., 2018b. Dynamic properties of calcareous and siliceous sands under isotropic and anisotropic stress conditions. Soils Found. 58, 172–184. https://doi.org/10.1016/j.sandf.2017.11.010.

Kalpakci, V., Bonab, A.T., Özkan, M.Y., Gülerce, Z., 2018. Experimental evaluation of geomembrane/geotextile interface as base isolating system. Geosynth. Int. 25. https://doi.org/10.1680/jgein.17.00025.

Kermani, B., Xiao, M., Stoffels, S.M., Qiu, T., 2018. Reduction of subgrade fines migration into subbase of flexible pavement using geotextile. Geotext. Geomembranes 46, 377–383. https://doi.org/10.1016/j.geotexmem.2018.03.006.

King, D.J., Bouazza, A., Gniel, J.R., Rowe, R.K., Bui, H.H., 2017. Serviceability design for geosynthetic reinforced column supported embankments. Geotext. Geomembranes 45, 261–279. https://doi.org/10.1016/j.geotexmem.2017.02.006.

Latha, G.M., AM, N.V., 2016. Static and cyclic load response of reinforced sand through large triaxial tests. Japanese Geotech. Soc. Spec. Publ. 2, 2342–2346.

Latha, G.M., Murthy, V.S., 2007. Effects of reinforcement form on the behavior of geosynthetic reinforced sand. Geotext. Geomembranes 25, 23–32. https://doi.org/10.1016/j.geotexmem.2006.09.002.

Latha, M.G., Murthy, V.S., 2006. Investigations on sand reinforced with different geosynthetics. Geotech. Test J. 29, 474–481. https://doi.org/10.1520/GTJ100439.

LaVielle, T.H., 2008. Liquefaction Susceptibility of Uncemented Calcareous Sands From Puerto Rico by cyclic triaxial testing. Ph.D. dissertation. Virginia Tech, Blacksburg, VA.

Liao, H.-J., Su, S.-F., 2012. Base Stability of Grout Pile-Reinforced Excavations in Soft Clay. J. Geotech. Geoenviron. Eng. 138, 184–192. https://doi.org/10.1061/(ASCE)GT.

Luo, F., Zhang, G., Liu, Y., Ma, C., 2018. Centrifuge modeling of the geotextile reinforced slope subject to drawdown. Geotext. Geomembranes 46, 11–21. https://doi.org/10.1016/j.geotexmem.2017.09.001.

Markou, I., 2016. Effect of Grain Shape and Size on the Mechanical Behavior of Reinforced Sand. Procedia Eng 143, 146–152. https://doi.org/10.1016/j.proeng.2016.06.019.

Markou, I.N., 2018. A Study on Geotextile — Sand Interface Behavior Based on Direct Shear and Triaxial Compression Tests. Int. J. Geosynth. Gr. Eng. 0, 0. https://doi.org/10.1007/s40891-017-0121-7.

Naeini, S.A., Gholampoor, N., 2014. Cyclic behaviour of dry silty sand reinforced with a geotextile. Geotext. Geomembranes 42, 611–619. https://doi.org/10.1016/j.geotexmem.2014.10.003.

Nguyen, M.D., Yang, K.H., Lee, S.H., Wu, C.S., Tsai, M.H., 2013. Behavior of nonwoven-geotextile-reinforced sand and mobilization of reinforcement strain under triaxial compression. Geosynth. Int. 20, 207–225.

Nicks, J.E., Esmaili, D., Adams, M.T., 2016. Deformations of geosynthetic reinforced soil under bridge service loads. Geotext. Geomembranes 44, 641–653. https://doi.org/10.1016/j.geotexmem.2016.03.005.

Nova-Roessig, L., Sitar, N., 2006. Centrifuge Model Studies of the Seismic Response of Reinforced Soil Slopes. J. Geotech. Geoenviron. Eng. 132, 388–400. https://doi.org/10.1061/(ASCE)1090-0241(2006)132:3(388.

Perkins, S.W., Cortez, E.R., 2005. Evaluation of base-reinforced pavements using a heavy vehicle simulator. Geosynth. Int. 12, 86–98. https://doi.org/10.1680/gein.2005.12.2.86.

Plácido, R., Portelinha, F.H.M., Futai, M.M., 2018. Field and laboratory time-dependent behaviors of geotextiles in reinforced soil walls. Geosynth. Int. 25, 215–229.

Portelinha, F.H.M., Zornberg, J.G., 2017. Effect of infiltration on the performance of an unsaturated geotextile-reinforced soil wall. Geotext. Geomembranes 45, 211–226. https://doi.org/10.1016/j.geotexmem.2017.02.002.

Rezvani, R., Shahnazari, H., Salehzadeh, H., Dehnavi, Y., 2011. The comparison of monotonic behaviors of two different calcareous sands. In: Proceeding of First International Conference on Geotechnique, Construction Materials and Environment, Mie, Japan, Nov, pp. 21–23.

Rowe, R.K., Liu, K.-W., 2015. Three-dimensional finite element modelling of a full-scale geosynthetic-reinforced, pile-supported embankment. Can. Geotech. J. 52, 2041–2054.

Rowe, R.K., Rentz, A.K., Brachman, R.W.I., Take, W.A., 2016. Effect of GCL type on downslope erosion in an exposed composite liner. J. Geotech. Geoenviron. Eng. 142, 1–10. https://doi.org/10.1061/(ASCE)GT.1943-5606.0001565.

Salem, M., Elmamlouk, H., Agaiby, S., 2013. Static and cyclic behavior of North Coast calcareous sand in Egypt. Soil Dynam. Earthq. Eng. 55, 83–91. https://doi.org/10.1016/j.soildyn.2013.09.001.

Saran, R.K., Viswanadham, B.V.S., 2018. Centrifuge model tests on the use of geosynthetic layer as an internal drain in levees. Geotext. Geomembranes 46, 257–276. https://doi.org/10.1016/j.geotexmem.2017.12.004.

Sayeed, M.M.A., Ramaiah, B.J., Rawal, A., 2014. Interface shear characteristics of jute/polypropylene hybrid nonwoven geotextiles and sand using large size direct shear test. Geotext. Geomembranes 42, 63–68. https://doi.org/10.1016/j.geotexmem.2013.12.001.

Shahnazari, H., Jafarian, Y., Tutunchian, M.A., Rezvani, R., 2016a. Undrained cyclic and monotonic behavior of hormuz calcareous sand using hollow cylinder simple shear tests. Int. J. Civ. Eng. 14, 209–219. https://doi.org/10.1007/s40999-016-0021-6.

Shahnazari, H., Jafarian, Y., Tutunchian, M.A., Rezvani, R., 2016b. Probabilistic Assessment of Liquefaction Occurrence in Calcareous Fill Materials of Kawaihae Harbor. Hawaii. Int. J. Geomech. 5016001. https://doi.org/10.1061/(ASCE)GM.1943-5622.0000621.

Shahnazari, H., Rezvani, R., 2013. Effective parameters for the particle breakage of calcareous sands: An experimental study. Eng. Geol. 159, 98–105. https://doi.org/10.1016/j.enggeo.2013.03.005.

Shahnazari, H., Salehzadeh, H., Rezvani, R., Dehnavi, Y., 2014. The effect of shape and stiffness of originally different marine soil grains on their contractive and dilative behavior. KSCE J. Civ. Eng. 18, 975–983. https://doi.org/10.1007/s12205-014-0286-8.

Sharma, S.S., Ismail, M.A., 2006. Monotonic and cyclic behavior of two calcareous soils of different origins. J. Geotech. geoenvironmental Eng. 132, 1581–1591.

Sommers, A.N., Viswanadham, B.V.S., 2009. Centrifuge model tests on the behavior of strip footing on geotextile-reinforced slopes. Geotext. Geomembranes 27, 497–505. https://doi.org/10.1016/j.geotexmem.2009.05.002.

Tizpa, P., Chenari, R.J., Fard, M.K., Machado, S.L., 2015. ANN prediction of some geotechnical properties of soil from their index parameters. Arab. J. Geosci. 8, 2911–2920.

Turker, E., Sadoglu, E., Cure, E., Uzuner, B.A., 2014. Bearing capacity of eccentrically loaded strip footings close to geotextile-reinforced sand slope. Can. Geotech. J. 51, 884–895. https://doi.org/10.1139/cgj-2014-0055.

Wang, H.-L., Chen, R.-P., Cheng, W., Qi, S., Cui, Y.-J., 2018. Full-scale model study on variations of soil stress in geosynthetic-reinforced pile-supported track-bed with water level change and loading cycles. Can. Geotech. J in press. https://doi.org/10.1139/cgj-2017-0689.

Xu, R., Fatahi, B., 2018. Influence of geotextile arrangement on seismic performance of mid-rise buildings subjected to MCE shaking. Geotext. Geomembranes 46, 511–528. https://doi.org/10.1016/j.geotexmem.2018.04.004.

Yang, K.-H., Zornberg, J.G., Liu, C.-N., Lin, H.-D., 2012. Stress distribution and development within geosynthetic-reinforced soil slopes. Geosynth. Int. 19, 62–78. https://doi.org/10.1680/gein.2012.19.1.62.

Zheng, Y., Fox, P.J., 2017. Numerical Investigation of the Geosynthetic Reinforced Soil–Integrated Bridge System under Static Loading. J. Geotech. geoenvironmental Eng. 143, 4017008.

Ziaie Moayed, R., Alibolandi, M., 2018. Effect of geotextile reinforcement on cyclic undrained behavior of sand. Soil Dynam. Earthq. Eng. 104, 395–402. https://doi.org/10.1016/j.soildyn.2017.11.013.

Zornberg, J.G., Arriag, F., 2003. Strain Distribution within Geosynthetic-Reinforced Slopes. J. Geotech. geoenviromental Eng. 129, 32–45. https://doi.org/10.1061/(ASCE)1090-0241(2003)129:1(32).

Zornberg, J.G., Portelinha, F.H.M., Bueno, B.S., 2013. Performance of nonwoven geotextile-reinforced walls under wetting conditions: laboratory and field investigations. Geosynth. Int. 20, 90–104. https://doi.org/10.1680/gein.13.00004.

Zornberg, J.G., Roodi, G.H., Gupta, R., 2017. Stiffness of Soil–Geosynthetic Composite under Small Displacements: I. Model Development. J. Geotech. Geoenviron. Eng. 143, 4017075. https://doi.org/10.1061/(ASCE)GT.1943-5606.0001768.